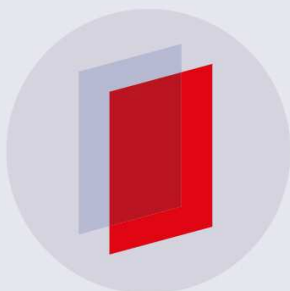


PAPER • OPEN ACCESS

## Search for ferroelectricity in fluoroperovskites: comparison between $\text{LiNiF}_3$ and $\text{NaNiF}_3$

To cite this article: A. C. Garcia-Castro *et al* 2019 *J. Phys.: Conf. Ser.* **1247** 012045

View the [article online](#) for updates and enhancements.



**IOP | ebooks™**

Bringing you innovative digital publishing with leading voices to create your essential collection of books in STEM research.

Start exploring the collection - download the first chapter of every title for free.

# Search for ferroelectricity in fluoroperovskites: comparison between $\text{LiNiF}_3$ and $\text{NaNiF}_3$

A. C. Garcia-Castro<sup>1</sup>, J. H. Quintero<sup>1</sup>, A. H. Romero<sup>2</sup>

<sup>1</sup>Department of Physics, Universidad Industrial de Santander, Carrera 27 Calle 9, 680002, Bucaramanga, Colombia.

<sup>2</sup>Department of Physics and Astronomy, West Virginia University, WV-26506-6315, Morgantown, USA.

E-mail: [acgarcia@uis.edu.co](mailto:acgarcia@uis.edu.co)

**Abstract.** Employing first-principles calculations, we have investigated the possible existence of the ferroelectric instability in the *G*-type antiferromagnetic  $\text{NaNiF}_3$  and  $\text{LiNiF}_3$  fluoroperovskites. The behavior of the unstable modes, at the cubic high-symmetry structure, is studied as a function of pressure. This study shows the vibrational landscape and define the conditions to drive the ferroelectricity in these materials, where the *A*-site dominates the polar instabilities.

## 1. Introduction

Ferroelectricity in perovskite oxides has attracted a huge interest going from fundamental studies to technological and industrial applications. Nowadays, its significance is even stronger because of the great challenge of finding materials that exhibits both ferroelectricity and magnetism—AFM or FM orderings—, mostly observed in the highly electronic correlated systems,  $\text{ABO}_3$  perovskites. Thus, the latter have been considered as the most attractive and promising candidates [1]. Interestingly, Scott and Blink have recently pointed out that multiferroism and magnetoelectricity can also be widely found in the leaved aside fluoride-based materials [2]. Examples of these systems recently studied are the multiferroics based-on Barium-fluorides  $\text{BaMF}_4$  ( $M = \text{Mn, Fe, Co, Ni}$ ) [3] that present a quasi-2D layer-by-layer structural octahedral arrangement. More recently, we demonstrated the existence of this multiferroic/magnetoelectric state in  $\text{BaCuF}_4$  with a larger Neel temperature, making of it a close-to-room temperature functioning system [4]. In the same direction,  $\text{NaMnF}_3$  was theoretically predicted [5, 6] and experimentally corroborated to be multiferroic under strain conditions [7].

Despite these efforts, ferroelectricity has been analyzed only in a few number of fluoride compounds with a remaining need for novel ferroelectrics. Thus, as one of the aims of our work is to explore and analyze possible polar ferroelectric instabilities in magnetic perovskite fluorides. In these systems, the physical phenomena such as superexchange interaction, stabilization of octahedral-tilting, and possible multiferroic or magnetoelectric behavior is still unclear. According to our previous discussion, we carried out a research, using first-principles calculations, on  $\text{NaNiF}_3$  and  $\text{LiNiF}_3$  fluoroperovskites in order to explore the possibility to include these materials as a new multiferroic.



## 2. Computational Details

Our density functional calculations of the electronic and structural properties were performed using the VASP code [8, 9]. PAW [10] pseudo-potentials were used to represent the valence and core electrons. The electronic configurations—for valence and semicore electrons—taken into account in the pseudo-potentials are Li ( $1s^2 2s^1$ ), Na ( $2p^6 3s^1$ ), Ni ( $3p^6 3d^8 4s^2$ ), and F ( $2s^2 2p^5$ ). The exchange correlation was represented within the GGA - PBEsol parametrization [11]. The magnetic character of these systems was included by the spin in the calculations by making the proper use of the exchange correlation (LSDA+ $U$ ). Due to the large  $d$ -electron localization, we corrected the high correlation by means of the DFT+ $U$  method [12] (GGA+ $U$ ,  $U = 4$  eV,  $J = 0$  eV), with a  $U$  value converged. The periodic solution of these crystalline structures was represented by using Bloch states with a Monkhorst-Pack  $k$ -point mesh of  $(8 \times 8 \times 8)$  and 700 eV energy cut-off, which has been tested already to give forces convergence to less than 0.0001 eV/Å and an error in total energy around  $\pm 0.4$  meV in all of the tested compound. Additionally, vibrational modes were fully converged with respect to energy and  $k$ -points mesh to obtain values in an error less than  $1 \text{ cm}^{-1}$ . Full phonon-dispersion curves were computed by calculating the dynamical matrix from the  $2 \times 2 \times 2$  supercell and mapped to the unit cell. The dynamical matrices and Born effective charges were obtained through the DFPT formalism [13] as implemented in VASP and post-processed with the Phonopy code [14].

## 3. Results and Discussion

In our previous studies [5], we demonstrated that the polar mode instability is present in several fluoroperovskite compounds. Nonetheless, this polar character disappears at the ground state and only non-polar structures remain. Therefore, the tuning and stabilization of such polar mode is crucial for the ferroelectricity survival. One way to achieve that is by understanding the vibrational behavior as a function of pressure. Therefore, we computed the phonon-dispersion curves at the cubic  $Pm\bar{3}m$  high-symmetry structure and analyzed the behavior of the modes as a function of pressure. Interestingly, in  $\text{NaNiF}_3$ , we found a total suppression of FE instability as a function of external pressure as shown in Figure 1. In Figure 1 is presented the squared frequency for all the unstable modes as a function of external pressure.

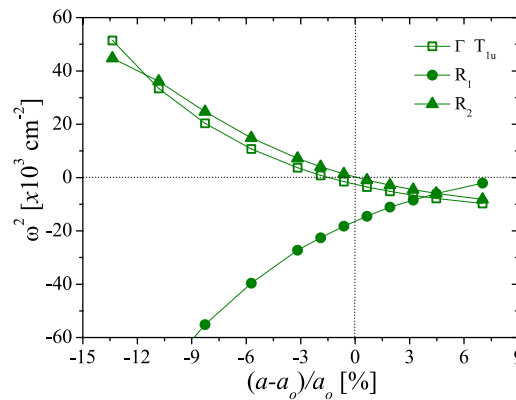


**Figure 1.** Behavior of FE and  $R$ -point instabilities as a function of hydrostatic pressure for  $\text{NaNiF}_3$ .

The total suppression of FE-instability at  $\Gamma$  is appreciated for strains above -2% with respect to the cubic relaxed lattice parameter. Additionally, the same behavior was observed for one of the instabilities located at  $R$ -point. The suppression of these instabilities is clearly different than those observed in other  $\text{NaBF}_3$  compounds previously discussed in Ref [5]. We noticed

that for this case, Ni possesses the smallest ionic radii in comparison with all others compounds that belong to the fluoroperovskites family in Ref. [5].

Figure 2 depicts the eigendisplacements as a function of hydrostatic pressure for three of polar modes at the zone-center  $\Gamma$ -point including the FE-instability. For this mode, no transition or considerable change in eigendisplacements were observed. While for the others two modes, a quasi-constant dependence was observed. Then, no anomalous trend responsible for transition of FE-mode was appreciated.

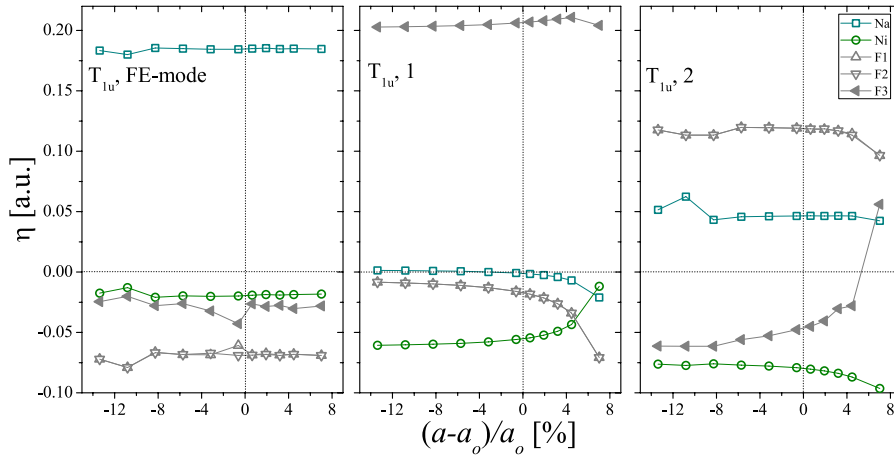


**Figure 2.** Eigendisplacements for all polar modes in NaNiF<sub>3</sub>.

In order to understand this behavior, we also analyzed the Born effective charges,  $Z^*$ , as a function of strain. A decrease of  $Z^*$  for Ni and F ions was observed at high expansion strain values going from  $2.21 e^-$  (in expansion) to  $1.65 e^-$  (in compression) and  $-1.84 e^-$  to  $-1.44 e^-$  for Ni and F respectively. A small fluctuation in the Born effective charges values are appreciated close to the eigendisplacements transition pressure. Up to this point, the previous results can be related to a different covalence bonding nature evidenced by the deviations in  $Z^*$ . Nonetheless, further studies are needed to find the origin of this out-of-trend behavior.

As we observed in our previous fluoroperovskites studies [5], the ionic  $A$  and  $B$  site radii size have a direct influence in the FE-instability. On the other hand, for the LiNiF<sub>3</sub> compound, we also computed the phonon-dispersion curves at the  $Pm\bar{3}m$  structure and extracted the information about the zone-boundary and the polar  $\Gamma$  modes respectively. From the theoretical analysis carried out, the LiNiF<sub>3</sub> compound was chosen due to its higher FE-instability,  $\omega = 224i \text{ cm}^{-1}$ . This compound presents a relaxed cubic lattice parameter of  $3.87 \text{ \AA}$  and its ferroelectric instability is higher than AFD-modes,  $214i \text{ cm}^{-1}$ ,  $166i \text{ cm}^{-1}$ ,  $213i \text{ cm}^{-1}$ , and  $190i \text{ cm}^{-1}$  for  $R_4^+$ ,  $R_5^+$ ,  $X_5^+$ , and  $M_3^+$  respectively. This observation explains why a stable ferroelectric ordering is observed at the relaxed ground state structure, where a  $R3c$  crystal symmetry type —like in LiNbO<sub>3</sub>— is expected, as also suggested in Ref. [15]. Figure 3 shows the instability analysis of the phonon modes as a function of strain at the Brillouin zone-center and boundary zone. For strain values lower than  $-3\%$  of the relaxed volume, the FE-instability shows the highest frequency value, even for the positive strain regime. However, below  $-4\%$  the AFD-instability becomes the dominant one in the vibrational landscape for this compound. The eigendisplacements for the FE-mode as a function of strain (see Figure 3) show an  $A$ -site dominated mode at the relaxed structure. For hydrostatic pressure, below the unconstrained volume, the influence of  $A$ -site decreases non-linearly and the mode begins to be dominated by  $B$ -site displacement. A sign change of the eigendisplacements was found at high strain of around  $-7\%$ . This behavior is similar such as the one observed previously in NaBF<sub>3</sub> [5].

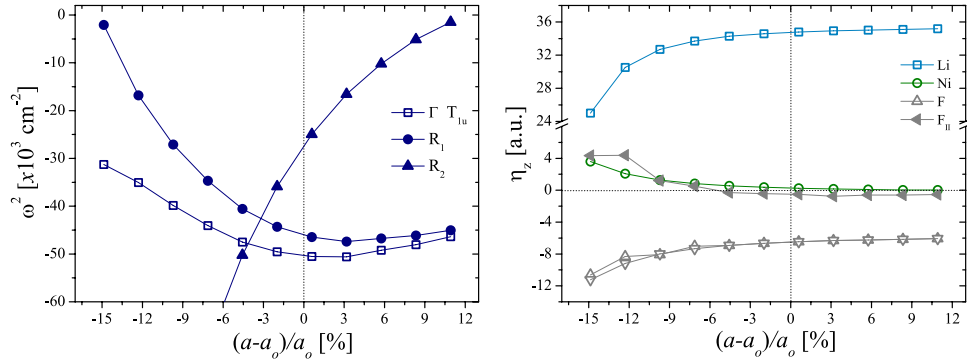


**Figure 3.** Squared frequency at the vibrational instabilities. We can observe the FE-mode at  $\Gamma$  and AFD-modes at  $R$ -point as a function of hydrostatic strain for  $\text{LiNiF}_3$  (left). Eigendisplacements of FE-mode instability in  $\text{LiNiF}_3$  are also shown (right).

Finally, when comparing  $\text{NaNiF}_3$  and  $\text{LiNiF}_3$ , it can be clearly observed that geometric conditions, based-on the  $A$ -site ionic radii, control the ferroelectricity appearance in these fluoroperovskites. Here, a polar ground state could be achieved for the smallest Li  $A$ -site compound, but is forbidden, and even the polar instability is suppressed by pressure, in the Na  $A$ -site case.

#### 4. Conclusions

We have studied, by means of first-principles calculations, the possible existence of a polar phase as a ground state in the  $\text{NaNiF}_3$  and  $\text{LiNiF}_3$ . We observed a suppression of FE instability for  $\text{NaNiF}_3$  as a function of pressure. However, it was not found a considerable change in the mode eigendisplacements with pressure. The compound  $\text{LiNiF}_3$  reveals a predisposition to ferroelectric behavior with a strong FE-mode instability in comparison to the others instabilities at the zone boundary in the phonon-dispersion. Then, the model for an  $A$ -site geometrically driven ferroelectricity in fluorides is corroborated. To expand the knowledge of this compound, future work can be focused in the understanding of the possible coupling between the FE-mode and the  $G$ -type AFM magnetic structure in  $\text{LiNiF}_3$  exploring the multiferroic/magnetoelectric phenomenon of this compound.

#### 5. Acknowledgments

This work used the XSEDE which is supported by National Science Foundation grant number ACI-1053575. The authors also acknowledge the support from the Texas Advances Computer Center (with the Stampede2 and Bridges supercomputers). This work was supported by the DMREF-NSF 1434897, NSF OAC-1740111 and DOE DE-SC0016176 projects.

#### References

- [1] Fiebig M 2005 *Journal of Physics D: Applied Physics* **38** R123–R152
- [2] Scott J F and Blinc R 2011 *Journal of physics. Condensed matter : an Institute of Physics journal* **23** 113202
- [3] Ederer C and Spaldin N A 2006 *Phys. Rev. B* **74**(2) 020401
- [4] Garcia-Castro A C, Ibarra-Hernandez W, Bousquet E and Romero A H 2018 *Phys. Rev. Lett.* **121**(11) 117601

- [5] Garcia-Castro A C, Spaldin N A, Romero A H and Bousquet E 2014 *Phys. Rev. B* **89**(10) 104107
- [6] Garcia-Castro A C, Romero A H and Bousquet E 2016 *Phys. Rev. Lett.* **116**(11) 117202
- [7] Yang M, KC A, Garcia-Castro A C, Borisov P, Bousquet E, Lederman D, Romero A H and Cen C 2017 *Scientific Reports* **7** 7182
- [8] Kresse G and Furthmüller J 1996 *Phys. Rev. B* **54** 11169–11186
- [9] Kresse G and Joubert D 1999 *Phys. Rev. B* **59**(3) 1758–1775
- [10] Blöchl P E 1994 *Phys. Rev. B* **50**(24) 17953–17979
- [11] Perdew J P, Ruzsinszky A, Csonka G I, Vydrov O A, Scuseria G E, Constantin L A, Zhou X and Burke K 2008 *Phys. Rev. Lett.* **100**(13) 136406
- [12] Liechtenstein A I, Anisimov V I and Zaanen J 1995 *Phys. Rev. B* **52**(8) R5467–R5470
- [13] Gonze X and Lee C 1997 *Phys. Rev. B* **55**(16) 10355–10368
- [14] Togo A, Oba F and Tanaka I 2008 *Phys. Rev. B* **78** 1–9
- [15] Claeysens F, Oliva J M, Sanchez-Portal D and Allan N L 2003 *Chem. Commun.* (19) 2440–2441